Magazine of Civil Engineering. 2019. 91(7). Pp. 121–128
Инженерно-строительный журнал. 2019. № 7(91). С. 121–128

Magazine of Civil Engineering

ISSN 2071-0305

journal homepage: http://engstroy.spbstu.ru/

DOI: 10.18720/MCE.91.11

An improved membrane element for high-rise building with shear walls

***Z.-Q. Liu*[a*], *J. Zhang*[b], *F. Li*[c], *H.-P. Jin*[a]. *Z.-Y. Zong*[a]**
[a] *Yancheng Institute of Technology, Yancheng, China*
[b] *Guizhou Minzu University, Guiyang, China*
[c] *Chongqing University, Chongqing, China*
** E–mail: zhaoqiuliu@sina.com*

Keywords: finite element method, structural design, numerical models, wall-beam connection, computational accuracy, high-rise building

Abstract. Although a high computational accuracy can be obtained when a membrane element with rotational degrees of freedom is used for the numerical analysis of wall-beam connection of high-rise building, this method often leads to some weak analysis results because of the vague relation between rotational degrees of freedom and displacement field compared with beam or slab element. In this paper, a constraint relation was established between the rotational displacement field with independent interpolation and the rotational angle of rigid body through adopting a penalty function method, and then an improved membrane element with rotational degrees of freedom was constructed based on the work of ALLMAN. The improved membrane element was added in the standard analysis module of ANSYS through using a second development interface named UPFs (User Programming Features). Also, a curved wall was adopted as the example to test the performance of improved membrane element. The preliminary results show the improved membrane element can pass most of patch tests with no extra zero energy mode. To further verify the performance of improved membrane element used for the analysis of wall-beam connection, a high-rise building with coupled shear walls was also adopted to compare the numerical analysis results produced by four different simulation elements. The results show the improved membrane element is a reliable and superior type with some advantages including simple data preparation, convenient programming and insensitive penalty parameter.

1. Introduction

In the numerical analysis of high-rise building, the development of simulation element for shear wall has experienced three stages including thin-walled bar, membrane and shell. In the practical application, a flat slab element that based on the theories of slab and membrane is often adopted in the finite element method to replace the shell element [1–4]. In the high-rise building with shear walls, except some arc-shaped walls for good appearance, most of shear walls often adopt flat shape. For the few arc-shaped walls, the refined flat slab element is often used to simulate the curved surface, and the calculation results are also more accurate when the element is refined enough [5–7].

Stiffness matrix is an essential characteristic of the simulation element, for the flat slab element, it is formed by superposing plane stress element and bending element. If adopting the linear superposition method formed by membrane and slab, two problems may be occur. One is the poor computational accuracy, although this problem can be solved by setting up rotational degrees of freedom or adding additional displacement shape function. The other is that no definite solution can be drawn for analyzing some shear wall structures as the membrane element that built by usual rotational degrees of freedom is combined with slab element [8–11].

Although ALLMAN membrane element has been widely used in the major finite element applications, a redundant zero-energy mode is often produced for the structural analysis, as well as the above two problems

Liu, Z.-Q., Zhang, J., Li, F., Jin, H.-P., Zong, Z.-Y. An improved membrane element for high-rise building with shear walls. Magazine of Civil Engineering. 2019. 91(7). Pp. 121–128. DOI: 10.18720/MCE.91.11

Лиу Ч.-К., Чанг Дж., Ли Ф., Джин Х.-П., Чонг Ч.-Ю. Мембранный элемент для высотных зданий связевой системы // Инженерно-строительный журнал. 2019. № 7(91). С. 121–128. DOI: 10.18720/MCE.91.11

[12–14]. To solve these problems, the ALLMAN membrane element was improved in this paper by using the User Programming Features (UPFs), which is a second development interface of ANSYS. A curved wall was adopted to test the performance of improved membrane element through setting in a FORTRAN subroutine in the standard analysis module of ANSYS. The test contents included eigenvalue inspection, fragmentation inspection, high-order fragmentation inspection, and coordination inspection of degrees of freedom. The preliminary results show the improved membrane element can pass most of patch tests and has a preferable computational accuracy when combining with slab element for the analysis of curved wall. To further confirm the analysis accuracy of improved membrane element used in the wall-beam connection, a high-rise building with coupled shear walls was analyzed by adopting four different simulation elements. The calculation results show the improved membrane element is a reliable and superior type with some advantages including simple data preparation, convenient programming and insensitive penalty parameter.

2. Methods

2.1. ALLMAN Membrane Element

To build the early membrane element with rotational degrees of freedom, engineers have paid more attention to the physical significance of rotational angle. The conventional practice is to set a cubic function for the additional displacement field of element. With using this method, however, some numerical experiments have proved that the matrix formula of membrane element is very complicated, and the computational accuracy is also not high. Many research works have been conducted to solve this problem during the past decades, and big progress has been achieved [15–19]. One of the most typical methods is the formation way of rotational degrees of freedom suggested by ALLMAN.

ALLMAN's method is suitable for triangular element shown in Figure 1. The accuracy of triangular element with rotational degrees of freedom is between linear strain triangular element with six nodes and constant strain triangular element with three nodes. The key to success of this method is to set up a reasonable relationship of node displacement between line midpoint and angular point.

Based on the work of ALLMAN, COOK expanded the formation way of rotational degrees of freedom from triangular element with three nodes to quadrilateral element with four nodes and arbitrary shape (shown in Figure 2) [20]. With high computational accuracy is the biggest advantage of this method compared with conventional membrane element with four nodes, and it can be easily combined with slab element with four nodes. As shown in Figure 3, however, a redundant zero-energy mode is often produced by using COOK's method. Therefore, the following parts of this paper focus on improving the ALLMAN membrane element and testing the application effects of improved membrane element.

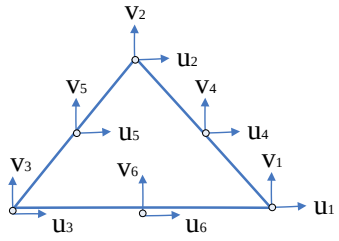

Figure 1. Triangle ALLMAN membrane element with three nodes.

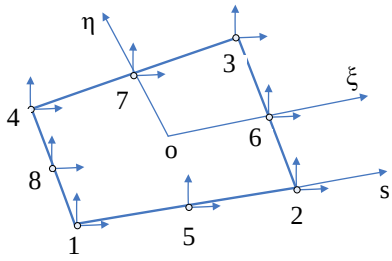

Figure 2. Quadrilateral membrane element with four nodes.

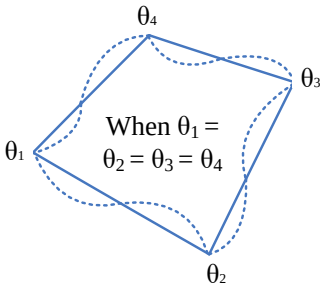

Figure 3. A redundant zero-energy mode of ALLMAN membrane element.

2.2. ALLMAN-based Improved Membrane Element

To solve the redundant zero-energy mode of ALLMAN membrane element and the problems addressed in the introduction, a penalty function method is adopted to represent the equivalence relation between the field of rotational degrees of freedom with independent interpolation and the rotational angle of rigid body in the element energy functional. The selected displacement field is shown as follows:

$$u = u_c + u_\lambda, \tag{1}$$

where u_c represents the bilinear compatible displacement field, and u_λ represents the incompatible displacement item. The rotational angle of rigid body of membrane element can be obtained from the theories of elastic mechanics, that is:

$$\omega^0 = \frac{1}{2}\left(-\frac{\partial}{\partial y} \quad \frac{\partial}{\partial x} \right) \begin{Bmatrix} u \\ v \end{Bmatrix} = D_2 \begin{Bmatrix} u \\ v \end{Bmatrix}. \tag{2}$$

Considering the equal relationship of rotational angle between node and rigid body, the energy functional can be represented as follows:

$$\prod = \int_V \frac{1}{2}\varepsilon^T C_1 \varepsilon dV + \int_V \frac{1}{2} C_2 \left(\omega^0 - \omega\right)^2 dV - W. \tag{3}$$

The matching stiffness matrix is:

$$K = \int_V \begin{bmatrix} B_c & B_\lambda \end{bmatrix}^T C_1 \begin{bmatrix} B_c & B_\lambda \end{bmatrix} dV + \int_V \begin{bmatrix} H_c & H_\lambda \end{bmatrix}^T C_2 \begin{bmatrix} H_c & H_\lambda \end{bmatrix} dV, \tag{4}$$

where $H_c = D_2^T N - N_\omega$, in the Cartesian coordinates:

$$D_2^T N = \begin{bmatrix} -\frac{\partial}{2\partial y} & \frac{\partial}{2\partial x} \end{bmatrix} \begin{bmatrix} N_1 & 0 & H_1 & N_2 & 0 & H_3 & N_3 & 0 & H_5 & N_4 & 0 & H_7 \\ 0 & N_1 & H_2 & 0 & N_2 & H_4 & 0 & N_3 & H_6 & 0 & N_4 & H_8 \end{bmatrix}. \tag{5}$$

A method of independent bilinear interpolation is adopted in the field of rotational degrees of freedom of node, that is:

$$\omega = \sum_1^4 N_i w_i = \begin{bmatrix} 0 & 0 & N_1 & 0 & 0 & N_2 & 0 & 0 & N_3 & 0 & 0 & N_4 \end{bmatrix} \{u\}_{12\times 1} = \begin{bmatrix} N_\omega \end{bmatrix} \{u\}_{12\times 1}. \tag{6}$$

The above method is also adopted for coordinate conversion between physical space and mapping space, namely:

$$\begin{Bmatrix} x \\ y \end{Bmatrix} = \begin{bmatrix} N_1 & 0 & N_2 & 0 & N_3 & 0 & N_4 & 0 \\ 0 & N_1 & 0 & N_2 & 0 & N_3 & 0 & N_4 \end{bmatrix} \begin{Bmatrix} x_1 \\ y_1 \\ x_2 \\ y_2 \\ x_3 \\ y_3 \\ x_4 \\ y_4 \end{Bmatrix}. \tag{7}$$

In the Formula 7, x_i and y_i (i = 1, 2, 3, 4) are coordinate values of four angular nodes in the Cartesian coordinate system. The partial derivatives of field variables are used in the calculation, which corresponds to x and y coordinates of physical space and ξ and η coordinates of mapping space respectively. Normally, the derivative for x and y coordinates is difficult to get. Therefore, the derivative for ξ and η coordinates can be obtained by using the derivability rule, namely:

$$\begin{Bmatrix} \frac{\partial \varphi}{\partial \xi} \\ \frac{\partial \varphi}{\partial \eta} \end{Bmatrix} = \begin{bmatrix} J \end{bmatrix} \begin{Bmatrix} \frac{\partial \varphi}{\partial x} \\ \frac{\partial \varphi}{\partial y} \end{Bmatrix}, \tag{8}$$

where $[J]$ represents the Jacobi matrix, and for slab element with four nodes, the following formula can be obtained easily:

$$\begin{Bmatrix} \frac{\partial \varphi}{\partial x} \\ \frac{\partial \varphi}{\partial y} \end{Bmatrix} = \begin{bmatrix} J \end{bmatrix}^{-1} \begin{Bmatrix} \frac{\partial \varphi}{\partial \xi} \\ \frac{\partial \varphi}{\partial \eta} \end{Bmatrix} = \frac{1}{|J|} \begin{bmatrix} J_{22} & -J_{12} \\ -J_{21} & J_{11} \end{bmatrix} \begin{Bmatrix} \frac{\partial \varphi}{\partial \xi} \\ \frac{\partial \varphi}{\partial \eta} \end{Bmatrix} = \begin{bmatrix} \Gamma_{11} & \Gamma_{12} \\ \Gamma_{21} & \Gamma_{22} \end{bmatrix} \begin{Bmatrix} \frac{\partial \varphi}{\partial \xi} \\ \frac{\partial \varphi}{\partial \eta} \end{Bmatrix}. \tag{9}$$

The correction matrix produced by compatible displacement is as follows:

$$H_c = D_2 \{u\} = \frac{1}{2} \begin{bmatrix} 0 & 0 & 0 & 0 \\ 0 & 0 & 0 & 0 \\ 0 & -1 & 1 & 0 \end{bmatrix} \begin{Bmatrix} u_{,x} \\ u_{,y} \\ v_{,x} \\ v_{,y} \end{Bmatrix}. \tag{10}$$

To make the element pass through the patch tests of displacement, a B-bar method is adopted to solve the $[H_\lambda]$ strain matrix [21]. Therefore, the solved strain matrix is described as follows $\left(H_{B-bar} = \int_V D_2^T M dV\right)$:

$$H_\lambda = D_2^T M - \frac{1}{V}\int_V D_2^T M dV. \tag{11}$$

Although the above improved membrane element can pass through the patch tests of displacement and no longer has a redundant zero-energy mode, it cannot pass through the patch tests of boundary. Therefore, the strain matrix that corresponds to displacement of coordination part should be further handled as follows:

$$G_{\theta M} = G_\theta - \frac{1}{V^e}\int_{V^e} G_\theta dv. \tag{12}$$

Based on the above formula, the improved membrane element not only can pass through the patch tests of displacement and boundary, but also can direct connect with the frame beam. However, the connection stiffness is too weak. So it is recommended to delete the displacement of incompatible part when the second part of stiffness matrix is calculated in formula (4), and the stiffness matrix of element adopts 3×3 way of Gauss integral. After the above amendments, the improved membrane element can achieve actual connection stiffness as direct connects with the frame beam. As shown in Figure 4, the element stiffness is calculated through a FORTRAN program, and the improved membrane element is planted into the software of ANSYS by the secondary development interface (namely, the UPFs).

```
*deck, UserElem   USERDISTRIB
      subroutine UserElem (elID, matID, keyMtx, lumpm, nDim, nNodes,
     &            Nodes, nIntPnts, nUsrDof, kEStress,
     &            KeyAnsMat, keySym, nKeyOpt, KeyOpt,
     &            temper, temperB, tRef, kTherm,
     &            nPress, Press, kPress, nReal, RealConst,
     &            nSaveVars, saveVars, xRef, xCur,
     &            TotValDofs, IncValDofs, ItrValDofs,
     &            VelValDofs, AccValDofs,
     &            kfstps, nlgeom, nrkey, outkey, elPrint, iott,
     &            keyHisUpd, Idstep, isubst, ieqitr, timval,
     &            keyEleErr, keyEleCnv,
     &            eStiff, eMass, eDamp, eSStiff,
     &            fExt, fInt, elVol, elMass, elCG,
     &            nRsltBsc, RsltBsc, nRsltVar, RsltVar,
     &            nElEng, elEnergy)
c*******************************************************
c
c*** Primary function: General User Element Subroutine
```

Figure 4. A user-defined subroutine.

3. Results and Discussion

3.1. Performance test for a curved wall

Based on the secondary development interface of UPFs provided by ANSYS, a curved wall (shown in Figure 5) is adopted as the example to test the performance of improved membrane element. The test contents include eigenvalue inspection, fragmentation inspection, high-order fragmentation inspection, and coordination inspection of degrees of freedom.

A concentrated force (100kN) is exerted on the upper two corner points of curved wall along the negative direction of X and Y-axes. Three types of grids including 3×5, 5×7 and 7×10 are calculated respectively, and the displacements of upper two corner points are listed in Table 1. To facilitate a comparative study, a shell element named SHELL63 is adopted in the software of ANSYS. The displacement shape function is represented by additional incompatible mode, and the ALLMAN method is used to form the rotational degrees of freedom. All the calculated results of displacements are shown in Table 1, it can be seen the calculated displacements of three types of grids are rather close.

Table 1. A comparison table for the calculated displacements of load point (Unit: mm).

Grid	improved membrane element		SHELL63 element of ANSYS	
	U_{x1}	U_{y2}	U_{x1}	U_{y2}
3×5	–2.558	–2.558	–2.4091	–2.4091
5×7	–2.582	–2.584	–2.4839	–2.4839
7×10	–2.594	–2.600	–2.5152	–2.5152

The preliminary results show the improved membrane element can pass most of patch tests with no extra zero-energy mode compared with traditional ALLMAN element. In addition, it can direct connect with frame beam element with no extra changes, and transfer forces accurately.

3.2. Case study for a high-rise building with coupled shear walls

The wall-beam connection is common in the high-rise building with shear walls. Therefore, to further verify the accuracy of improved membrane element used for the analysis of wall-beam connection, a high-rise building with coupled shear walls is adopted (shown in Figure 6). The concrete strength grade of shear wall is C25 (Chinese standard, which represents the compressive strength standard value of concrete cube is 25 N/mm^2), and the thickness of shear wall is 200 mm. With 3 m storey height, the opening height of shear wall is 2.4 m, and the height of coupling beam located in middle layers is 0.6 m. A horizontal concentrated load (200 kN) is applied to the position of each floor height respectively. Four different simulation elements are adopted as follows to calculate this high-rise building with coupled shear walls. (1) Opening hole is adopted on shear wall to create coupling beam, and shell element is used to simulate wall-column and wall-beam (shell-shell); (2) The coupling beam is created in the manner of frame structure, and constrain equation is adopted to simulate the continuous relationship of rotational angles between beam and shell (shell-beam); (3) The coupling beam is also created in the manner of frame structure, and penalty element is adopted to simulate the continuous relationship of rotational angles between beam and shell (SATWE uses this method, which is a Chinese finite element analysis software); (4) The coupling beam is still created in the manner of frame structure, and the improved membrane element is adopted to simulate the continuous relationship of rotational angles between beam and shell (this paper).

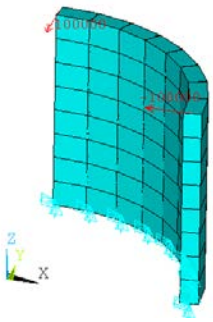

Figure 5. A structural model of curved wall.

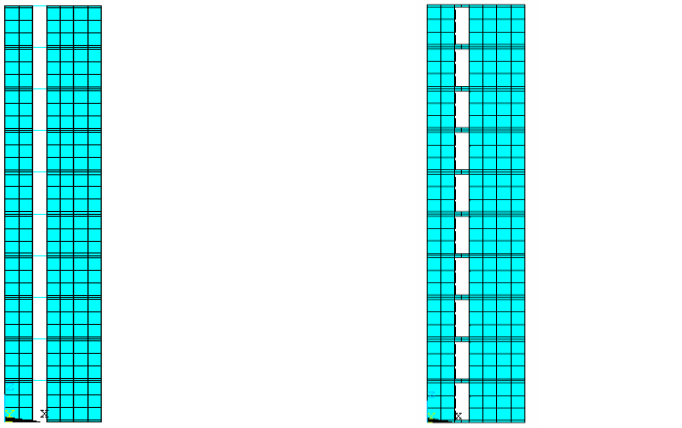

a) Modeling by frame beam b) Modeling by shear wall with openings

Figure 6. A model of high-rise building with coupled shear walls.

To avoid drawing a one-sided conclusion, three models with different span-depth ratios are designed. The span-depth ratios vary from 2, 4 to 6 by keeping unchanged section height of wall and column and increasing the width of opening. The calculated results show that displacement, shear force, and bending moment of each layer with different span-depth ratios are rather close. Among them, the results of constrain equation and shell element are closest, and the connection strength of wall-beam of improved membrane element is slightly soft. From Figure 7 to Figure 9 show the comparison of calculation results of displacement, shear force, and bending moment.

4. Conclusions

1. Based on the amendment of ALLMAN membrane element, an improved membrane element was proposed in this paper to solve the problems including redundant zero-energy mode, poor computational accuracy and ambiguous solution, which often occur when the traditional ALLMAN membrane element is used for the structural analysis of high-rise building with shear walls.

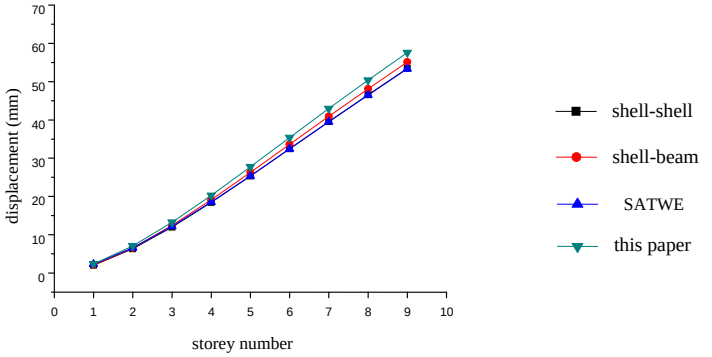

a) The span-depth ratio is 2

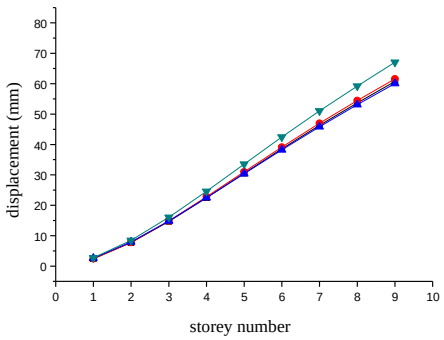

b) The span-depth ratio is 4

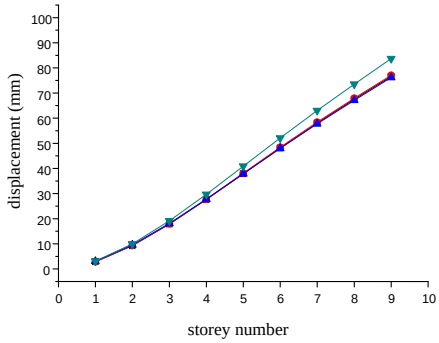

c) The span-depth ratio is 6

Figure 7. Comparison chart of displacement of each layer with different span-depth ratios.

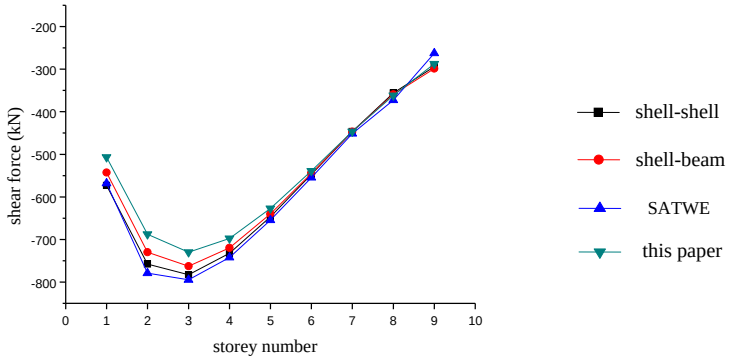

a) The span-depth ratio is 2

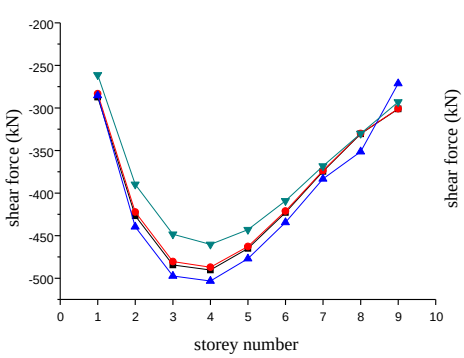

b) The span-depth ratio is 4

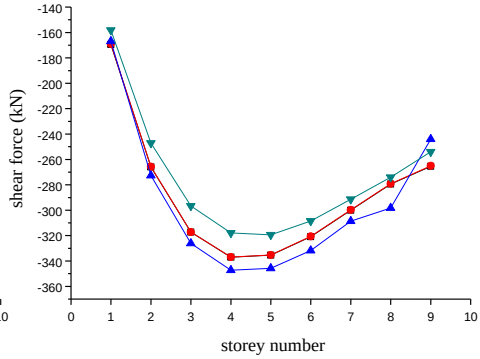

c) The span-depth ratio is 6

Figure 8. Comparison chart of shear force of each layer with different span-depth ratios.

2. By using the UPFs (User Programming Features, a second development interface), a FORTRAN subroutine of improved membrane element was added in the standard analysis module of ANSYS. A curved wall was adopted to test the performance of improved membrane element for structural component. The preliminary results show the improved membrane element can pass most of patch tests with no extra zero-energy mode compared with traditional ALLMAN membrane element.

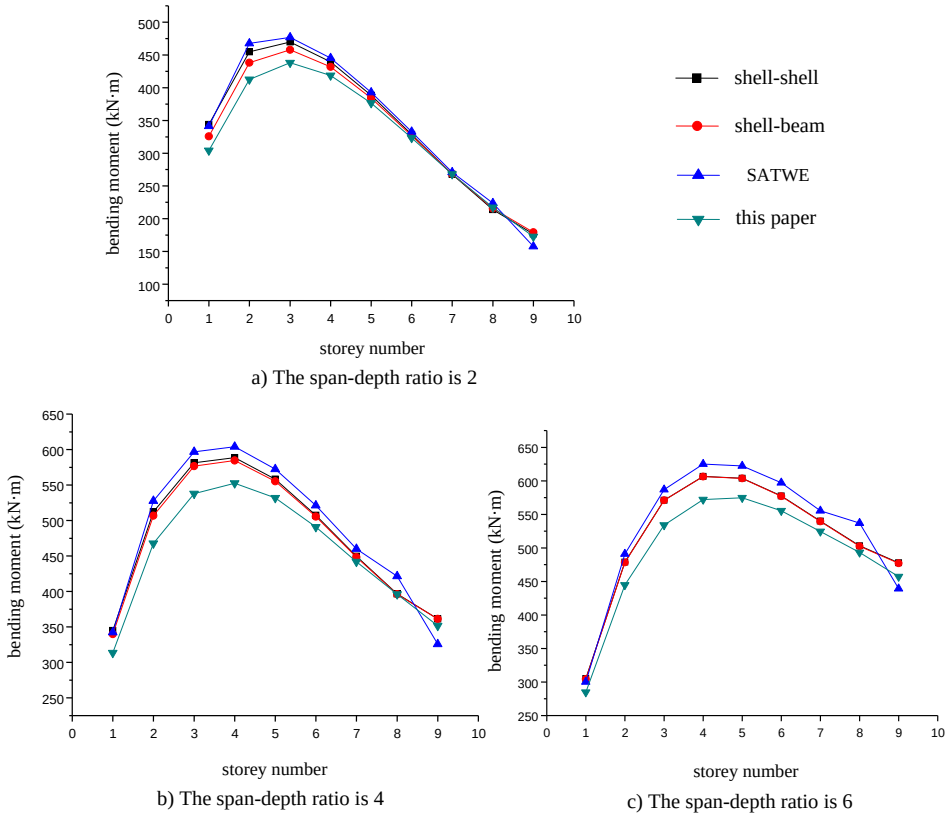

Figure 9. Comparison chart of bending moment of each layer with different span-depth ratios.

3. A high-rise building with coupled shear walls was also adopted to test the performance of improved membrane element for wall-beam connection. The results show the improved membrane element has preferable computational accuracy compared with other methods for the analysis of wall-beam connection, and is a reliable and effective type.

4. On the basis of UPFs function of ANSYS platform, currently only the preprocessor module including modeling, meshing, static and dynamic solver can be used to invoke the key data of displacement, stress and period. Since the postprocessor module of ANSYS cannot be fully used, the following work aims to improve the access of postprocessor module and take advantage of the powerful post-processing capacities.

References

1. Kim, H.S., Lee, D.G. Analysis of Shear Wall with Openings Using Super Elements. Engineering Structures. 2003. 25(8). Pp. 981–991. DOI: 10.1016/S0141-0296(03)00041-5
2. Kim, H.S., Lee, D.G., Kim, C.K. Efficient Three-dimensional Seismic Analysis of a High-rise Building Structure with Shear Walls. Engineering Structures. 2005. 27(6). Pp. 963–976. DOI: 10.1016/j.engstruct.2005.02.006
3. Worsak, K.N. A Simple and Efficient Finite Element for General Shell Analysis. International Journal for Numerical Methods in Engineering. 1979. 14(2). Pp. 179–200. DOI: 10.1002/nme.162014020
4. Lu, X.Z., Xie, L.L., Guan, H. A Shear Wall Element for Nonlinear Seismic Analysis of Super-tall Buildings Using OpenSees. Finite Elements in Analysis and Design. 2015. No. 98. Pp. 14–25. DOI: 10.1016/j.finel.2015.01.006
5. Bozdogan, K.B., Ozturk, D. Vibration Analysis of Asymmetric Shear Wall and Thin Walled Open Section Structures Using Transfer Matrix Method. Structural Engineering and Mechanics. 2009. 33(1). Pp. 95–107. DOI: 10.12989/sem.2009.33.1.095
6. Li, Y.G., Nie, Q. The Short-leg Shear Wall Element Based on the Analytical Trial Function Method. Engineering Mechanics. 2009. 26(4). Pp. 181–186. DOI: 10.1109/CLEOE-EQEC.2009.5194697
7. Ding, J.G., Zhu, Y. An Elastic-plastic Analysis of Short-leg Shear Wall Structures During Earthquakes. Earthquake Engineering and Engineering Vibration. 2012. 11(4). Pp. 525–540. DOI: 10.1007/s11803-012-0139-8
8. Pekau, O.A., Huttelmaier, H.P. A Versatile Panel Element for the Analysis of Shear Wall Structures. Computers and Structures. 1980. 12(3). Pp. 349–359. DOI: 10.1016/0045-7949(80)90032-2
9. Cheng, M.Y., Fikri, R., Chen, C.C. Experimental Study of Reinforced Concrete and Hybrid Coupled Shear Wall Systems. Engineering Structures. 2015. 82(1). Pp. 214–225. DOI: 10.1016/j.engstruct.2014.10.039
10. Cen, S., Zhou, M.J., Fu, X.R. A 4-node Hybrid Stress-function (HS-F) Plane Element with Drilling Degrees of Freedom Less Sensitive to Severe Mesh Distortions. Computers and Structures. 2011. 89(5). Pp. 517–528. DOI: 10.1016/j.compstruc.2010.12.010
11. Jalali, A., Dashti, F. Nonlinear Behavior of Reinforced Concrete Shear Walls Using Macroscopic and Microscopic Models. Engineering Structures. 2010. 32(9). Pp. 2959–2968. DOI: 10.1016/j.engstruct.2010.05.01
12. Chen, H.C. Evaluation of Allman Triangular Membrane Element Used in General Shell Analyses. Computers and Structures. 1992. 43(5). Pp. 881–887. DOI: 10.1016/0045-7949(92)90302-G

13. Allman, D.J. A Compatible Triangular Element Including Vertex Rotations for Plane Elasticity Analysis. Computers and structures. 1984. 19(2). Pp. 1–8. DOI: 10.1016/0045-7949(84)90197-4
14. Tian, R., Yagawa, G. Allman's Triangle Rotational DOF and Partition of Unity. International Journal for Numerical Methods in Engineering. 2007. 69(4). Pp. 837–858. DOI: 10.1002/nme.1790
15. Robinson, J. Four-node Quadrilateral Stress Membrane Element with Rotational Stiffness. International Journal for Numerical Methods in Engineering. 1980. 15(10). Pp. 1567–1569. DOI: 10.1002/nme.1620151012
16. Paknahad, M., Noorzaei, J., Jaafar, M.S. Analysis of Shear Wall Structure Using Optimal Membrane Triangle Element. Finite Elements in Analysis and Design. 2007. 43(11). Pp. 861–869. DOI: 10.1016/j.finel.2007.05.010
17. Sze, K.Y., Pan, Y.S. Hybrid Stress Tetrahedral Elements with Allman's Rotational D.O.F.s. International Journal for Numerical Methods in Engineering. 2000. 48(7). Pp. 1055–1070. DOI: 10.1002/(SICI)1097-0207(20000710)48:73.0.CO;2-P
18. Wen, Y., Zeng, Q.Y. Algorithm for Deriving Explicitly the Analytical Expression of Geometric Sstiffness Matrix of the 4-node, 24 Degrees of Freedom Flat Shell Element. Chinese Journal of Computational Mechanics. 2013. 30(6). Pp. 796–801. DOI: 10.7511/jslx201306008
19. Rebiai, C., Belounar, L. A New Strain Based Rectangular Finite Element with Drilling Rotation for Linear and Nonlinear Analysis. Archives of Civil and Mechanical Engineering. 2013. 13(1). Pp. 72–81. DOI: 10.1016/j.acme.2012.10.001
20. Cook, R.D. On the Allman Triangular and a Related Quadrilateral Elemen. Computers and structures. 1986. 22(6). Pp. 1065–1067. DOI: 10.1016/0045-7949(86)90167-7
21. Reissner, E. A Note on Variational Principles in Elasticity. International Journal of Solids and Structures. 1965. 1(1). Pp. 93–95. DOI: 10.1016/0020-7683(65)90018

Contacts:

Zhao-Qiu Liu, +86(0515)88168215; zhaoqiuliu@sina.com
Ji Zhang, +86(0851)83613490; jizhang@163.com
Feng Li, +86(023)65120720; 773859023@qq.com
Hao-Peng Jin, +86(0515)88168215; 2812706964@qq.com
Zhen-Yu Zong, +86(0515)88168215; 1642833684@qq.com